Pin-on-Plate vs. Pin-on-Disk Wear Tests: Theoretical and Numerical Observations on the Initial Transient Phase

Francesca Di Puccio *, Andrea Di Pietro , Lorenza Mattei

Posted Date: 11 March 2024

doi: 10.20944/preprints202403.0646.v1

Keywords: wear test; pin-on-plate; pin-on-disc; flat-on-disc; wear factor; Archard's wear law; wear predictive model

Article

Pin-on-Plate vs. Pin-on-Disk Wear Tests: Theoretical and Numerical Observations on the Initial Transient Phase

Francesca Di Puccio *, Andrea Di Pietro and Lorenza Mattei

Dip. Ingegneria Civile e Industriale, Università di Pisa; andrea.dipietro@phd.unipi.it; lorenza.mattei@unipi.it
* Correspondence: francesca.di.puccio@unipi.it; Tel.: +39 50 2218076

Abstract: Pin-on-plate and pin-on-disk wear tests are typically used for assessing the wear behavior of a given material coupling. Such a behavior is frequently described by a wear coefficient k, which is estimated, according to the Archard's law, as the ratio between the measured wear volume V and the product of the applied normal force F and the sliding distance s, i.e. $k=V/(F\ s)$. This study demonstrates that such a relationship is correct for pin-on-plate but not for pin-on-disk, particularly for flat-ended pins. Both analytical and finite element models of the two tests were developed, considering three different distances pin-disk axis. As results, wear volumes, pressure and wear depth maps were examined and compared for the same sliding distance. Though this study is focused only on the initial transient part of the wear tests, some interesting aspects arose: i) rotational effect in pin-on-disk tests affects k estimation, especially when the pin is near to the disk axis; ii) a simple analytical function is defined to correct the wear volume estimation for pin-on-disk tests; iii) due to the different sliding distances of contact points in pin-on-disk tests, pressure redistribution occurs with higher values on the inner side (closer to disk axis); the opposite trend is observed in wear depth maps. From a computational point of view, the pin-on-disk problem, only apparently simple, required very small time increments to correctly describe the circular trajectories of points, with high computational costs. Numerical strategies are currently under investigation to extend the study to the steady state phase of both tests.

Keywords: wear test; pin-on-plate; pin-on-disc; flat-on-disc; wear factor; Archard's wear law; wear predictive model

1. Introduction

Wear is a phenomenon as complex as it is widespread in everyday life. It can be observed in shoes, teeth, brakes and in many other elements. From an engineering point of view, it is important to consider wear when designing mechanical components and this requires an estimation of their wear resistance. Experimental tests are carried out at this purpose. Since this phenomenon is affected by many factors as materials properties, kinematic and loading conditions and so on, which can hardly be reproduced in laboratory, such tests most frequently apply simplified conditions. The two most common wear tests are performed on Pin-on-Plate (PoP) or Pin-on-Disk (PoD) apparati.

Pin-on-Plate wear tests are used to study reciprocating sliding wear and fretting. In both cases, a pin is loaded against a flat surface in presence of reciprocating motion; depending on the stroke length, sliding and fretting conditions are distinguished, the former having a wide stroke, much longer than the contact width, and the latter a small stroke, typically of the order of magnitude of the contact width. A schematic view of the two wear tests is given in Figure 1(a). These tests are well described in the ASTM-G133 [1] and D4170 [2], respectively.

Pin-on-disk wear tests reproduce continuous sliding contact conditions between a rotating disk and pin located at a given distance from the disk axis, as represented in fig. Figure 1(b). For PoD wear tests, the standard commonly adopted is ASTM-G99 [1].

 doi:10.20944/preprints202403.0646.v1

Both in PoP and PoD tests, two cases can occur: only one body wears out, i.e. the pin or the plate/disk, or both contact surfaces wear. According to the standards, the tests output are the wear volumes of each component measured directly (by means of gravimetric method) or, more often, computed from measurements of the worn scar and initial unworn pin geometry [1–3].

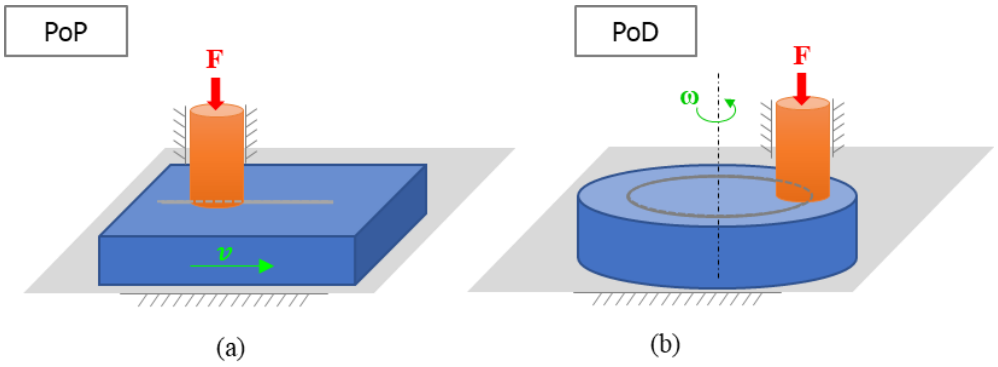

Figure 1. Schemes of Pin-on-Plate (PoP) (a) and Pin-on-Disk (PoD) (b) wear tests.

These experimental wear volumes are used to compute the wear coefficient k that characterizes the wear rate of the tribo-pair and is useful to compare material couplings, and also to calibrate numerical wear models [4–7]. The wear coefficient is commonly estimated according to the Archard wear law [8,9], i.e.

$$V = k\ F\ s, \tag{1}$$

stating that the wear volume V is proportional to the normal load **F** and the sliding distance s. In wear tests, F and s are imposed whilst the worn mass or volume is measured, so that the wear coefficient can be calculated as

$$k = V/(F\ s). \tag{2}$$

In the literature, Eq.(2) is used to estimate k from PoP and PoD wear tests, as reported in very recent experimental studies both on unilateral [4,10,11] and bilateral [5,12,13] wear. However, eq. (2) holds only for a translating body under constant load, and thus while it is correct for PoP wear tests, it provides only an approximation of k for PoD tests where a relative rotation pin-disk occurs. Nevertheless, to the best of author knowledge such equation has never been revised for the case of PoD wear tests.

This study compares PoP and PoD wear tests by means of both analytical and numerical FE models considering the real contact conditions and thus applying the Archard wear law in local instantaneous form. The final aim is to investigate how the rotational effect in PoD tests affects the estimation of k by varying the distance between pin axis and disk axis.

2. Materials and Methods

To compare the PoP and PoD wear tests, firstly Finite Element (FE) models were developed in Ansys®. Then, to clarify and generalize numerical results, the pertinent analytical relationships were formulated and solved in Matlab.

2.1. Test Cases

In the examined test cases, a cylindrical flat pin having radius r_p=5 mm was assumed to be in contact with the plane surface of a plate or a disc (Figures 1 and 2). For the PoD test, three conditions were examined differing in the distance R_d between the pin and disk axes, i.e. R_d= 1.25-2.5-5 r_p . All the bodies were assumed to be made of structural steel, with Young modulus of 200 GPa and Poisson ratio equal to 0.3. However, only the pin was considered as affected by wear, with a wear coefficient

Preprints.org (www.preprints.org) | NOT PEER-REVIEWED | Posted: 11 March 2024 doi:10.20944/preprints202403.0646.v1

k=1.25 10^{-7} mm²/N, value taken from the reference [14]. A 21 N normal load was applied to the pin and the same final sliding distance s_f corresponding to 1 round of the highest R_d (s_f=10 π r_p=157.08 mm) was simulated for both PoP and PoD cases.

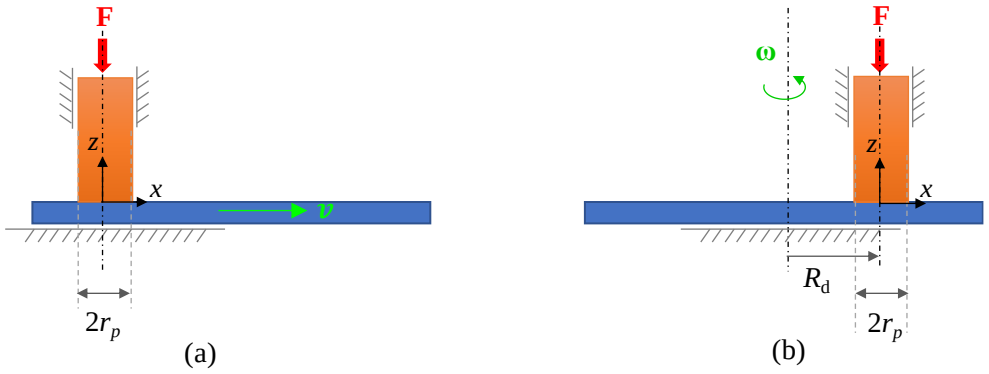

Figure 2. Schemes of the simulated PoP (a) and PoD (b) wear tests with the boundary conditions adopted in respective FE models.

2.2. Finite Element Models

The FE simulations were performed in Ansys Workbench® 2023, taking advantage of the dedicated tool for wear assessment.

2.2.1. Geometry and Materials

To simplify the analyses, the plate and the disk were treated as rigid bodies, only the pin was considered deformable and affected by wear.

2.2.2. Mesh

The cylinder was meshed with 3D prism (WED6) elements by employing the "Sweep method" while the plate/disc surface with TRI3 (3 nodes linear triangle) 2D elements (Figure 3). The contact surfaces were meshed with CONTA174 and TARGE170 elements (see Sec. 2.2.3)

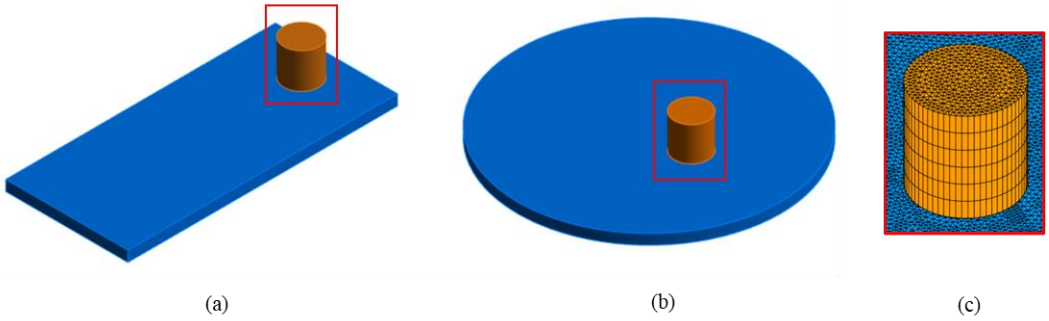

Figure 3. FE model of PoP (a) PoD (b) wear tests and details on the mesh (c).

2.2.3. Contact and Wear Conditions

The contact was assumed as asymmetric as in this case only one body wears out. Moreover, the contact was simulated as frictionless, since the effect of the friction on wear is negligible as demonstrated in [15]. The analysis was solved by means of an Augmented Lagrange algorithm and the nodal-projected normal from contact was adopted as detection method with the cylinder and plate/disk as contact and target body, respectively.

The wear behavior was activated through an APDL command script inserted in the contact section and calling the Ansys tool which applies the Archard's wear law in the generalized form

 doi:10.20944/preprints202403.0646.v1

$$\dot{h} = \frac{k}{H}\, p^m v^n, \tag{3}$$

where H is the material hardness, k is the wear coefficient, and m and n exponents of pressure and sliding velocity, respectively. In particular, the command TB WEAR with option ARCD was used for applying Eq. (3); TBDATA command was used to set the parameters of Eq.(3) and the TBFIELD command for selecting the time instants during which activate or deactivate wear. Parameters were set as H=m=n=1, so that the traditional form of the Archard wear law was adopted according to Eq.(1).

2.2.4. Boundary Conditions

The vertical load of 21 N was applied to the pin, which could only translate in the vertical direction to keep the contact with the counterpart. The motion was applied to the plate and the disk a translation of s in the first case and a rotation Θ in the second one. This small displacement was considered to limit the computational time below 4 hours using a processor Intel(R) Xeon(R) Silver 4214R CPU @ 2.40GHz with 64 GB RAM.

2.2.5. Analysis Settings

The time increment was set to 10^{-4} to 2.5 10^{-2} s which allowed to discretize the arc length with the chord along the node trajectories with a maximum error of 0.1%, making the computational time affordable.

2.3. Analytical Approach

The analytical description of both tests moves from the local instantaneous form of the Archard's law that can be rewritten as

$$\dot{h}(P,t) = k\, p(P,t)\, v(P,t), \tag{4}$$

relating the wear depth rate at a point P to the pressure p and sliding speed v both varying with time and point. The wear depth at a given instant is simply obtained integrating Eq.(4)

$$h(P,t) = k \int_0^t p(P,\tau)\, v(P,\tau)\, d\tau. \tag{5}$$

Accordingly, the wear volume is calculated as

$$V = k \int_A \int_0^t p(P,\tau)\, v(P,\tau)\, d\tau\, dA = k \int_0^t \left(\int_{A(t)} p(P,\tau) v(P,\tau)\, dA \right) d\tau. \tag{6}$$

In PoP tests, we can neglect the wear produced when reversing the motion and consider that the speed v is uniform and constant, therefore it can be written:

$$V_{PoP} = k\, v \int_A \int_0^t p(P,\tau)\, d\tau\, dA = k\, F\, v\, t = k\, F\, s. \tag{7}$$

Rather interestingly, the wear volume in PoP tests does not depend pressure distribution, i.e. on the shape of the pin, flat-ended or hemispherical.

On the other hand, when we consider a PoD test, the relative motion of the pin with respect to the disk is a rotation about the disk axis of an angle Θ. Therefore, the sliding distance of each point P, s_P, is proportional to the radial distance R of P from the disk axis (Figure 4), i.e.

 doi:10.20944/preprints202403.0646.v1

$$s_P = R\ \Theta. \tag{8}$$

Introducing the angular speed of the disc ω, assumed constant for simplicity, and substituting $\Theta = \omega\ t$, Eq.(5) becomes

$$h(P,t) = k\ \omega \int_0^t R\ p(P,\tau)\ d\tau. \tag{9}$$

Another difference between PoP and PoD models is that in the latter one the wear volume depends on pressure distribution, as Eq.(7) cannot be exploited

$$V_{PoD} = k\ \omega \int_A \int_0^t R\ p(P,\tau)\ d\tau\ dA = k\ \omega \int_0^t \left(\int_{A(t)} R\ p(P,\tau)\ dA \right) d\tau, \tag{10}$$

In the present study, for a flat ended pin and a low friction, we assumed that in the initial part of the test, pressure remained almost uniform $\underline{p} = F/(r_p^2 \pi)$ and the contact area constant. Therefore, the main difference between the two tests lies in the sliding distance.

Thus, we can write:

$$V_{PoD} = k \frac{F}{r_p^2 \pi}\ \omega \int_0^t \left(\int_A R\ dA \right) d\tau = k \frac{F}{r_p^2 \pi}\ \omega\ t \int_A R\ dA = k \frac{F}{r_p^2 \pi}\ \Theta \int_A R\ dA\ , \tag{11}$$

being $\Theta = s/R_d$ with s equal to the arc described by the center of the pin.

Equation (11) requires further manipulation of the integral

$$\int_A R\ dA = \int_{R_m}^{R_M} \int_{-\varphi(R)}^{\varphi(R)} R\ R\ d\varphi\ dR, \tag{12}$$

with

$$\varphi(R) = acos\left(\frac{R_d^2 + R^2 - r_p^2}{2\ R_d\ R}\right),\ R_m = R_d - r_p,\ R_M = R_d + r_p. \tag{13}$$

With few passages, being

$$\int_A R\ dA = 2 \int_{R_m}^{R_M} R^2\ \text{acos}\left(\frac{R_d^2 + R^2 - r_p^2}{2\ R_d\ R}\right) dR, \tag{14}$$

we obtain

$$V_{PoD} = k\ Fs\ \frac{2 \int_{R_m}^{R_M} R^2 \text{acos}\left(\frac{R_d^2 + R^2 - r_p^2}{2\ R_d\ R}\right) dR}{R_d\ r_p^2 \pi} \tag{15}$$

Preprints.org (www.preprints.org) | NOT PEER-REVIEWED | Posted: 11 March 2024 doi:10.20944/preprints202403.0646.v1

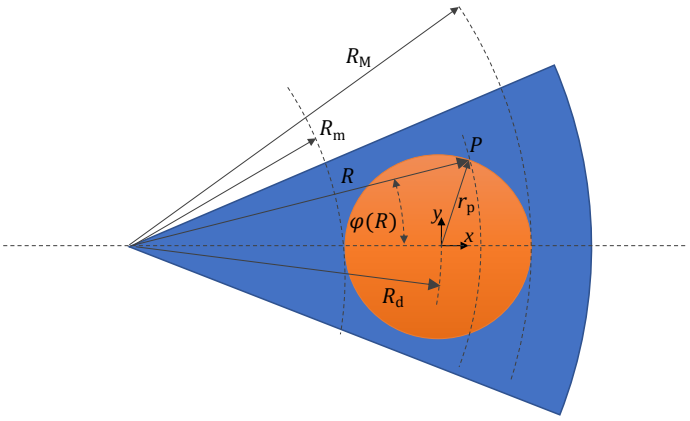

Figure 4. Main geometrical parameters used in Equations (9-15).

The last term on the right is dimensionless, depends on the geometry of the system and is typically omitted in the literature, for example when using PoD tests for evaluating k. We can consider that $g(\gamma)$ as the ratio between PoD and PoP wear volumes, when a uniform pressure distribution is considered. It can be expressed as a function of a dimensionless geometric parameter $\gamma = r_p/R_d$

$$g(\gamma) = 2\,\frac{\int_{1-\gamma}^{1+\gamma} \rho^2 \mathrm{acos}\left(\frac{1+\rho^2-\gamma^2}{2\,\rho}\right) d\rho}{\gamma^2\pi}\,, \qquad \rho = \frac{R}{R_d} \tag{16}$$

Its trend is shown is Figure 5 for $0 < \gamma < 1$, that is a limited range of practical values of γ. It is preferred to its inverse $\frac{R_d}{r_p}$ that should be considered in the field [1,∞). It is worth stressing that when $\gamma \to 0$, i.e. $\frac{R_d}{r_p} \to \infty$, the PoD →PoP.

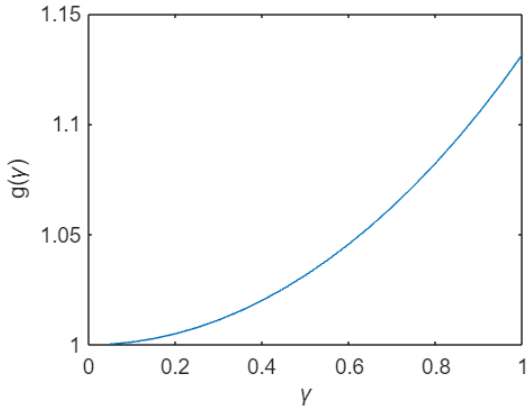

Figure 5. Trend of the function $g(\gamma)$ of Equation (14).

From Eq. (16), it can be observed that the ratio is maximum when γ=1, and $g(1)$=32/(9 π) ≅ 1.132, meaning that the PoD produced higher wear volumes than PoP over the same sliding distance when pressure can be considered uniform, as in the initial part of a test, until wear affects the geometry of the contact surface.

The above equations were implemented in a Matlab® script for estimating the wear volumes with a constant pressure approximation and compare it with FE results in a short sliding distance.

3. Results

The FE simulations of the four cases, one PoP and three track radii PoD, were completed and as results the wear volumes and the maps of the contact pressure and wear depth over the contact area

Preprints.org (www.preprints.org) | NOT PEER-REVIEWED | Posted: 11 March 2024 doi:10.20944/preprints202403.0646.v1

were analyzed. They are discussed for increasing values of the parameter γ, considering that $\gamma \to 0$ represents the PoP test, $\gamma = 0.2, 0.4$ and 0.8 the PoD cases with decreasing R_d= 5, 2.5 and 1.25 r_p respectively.

Figure 6 shows the trends of the wear volumes over the sliding distance, obtained from FE analyses. It can be observed that they are almost linear and that the PoP case has the lowest volume, slightly smaller than PoD γ=0.2–0.4, while the PoD γ=0.8 (smallest radius R_d) has the highest one.

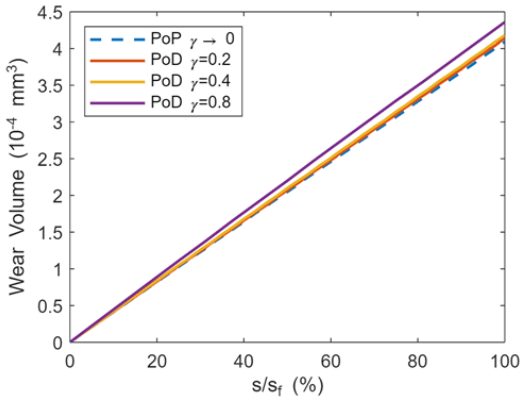

Figure 6. Wear volumes predicted by the FE vs. sliding distance, s_f=157.08 mm.

Differences in FE and analytical volumes can be easily appreciated from histograms in Figure 7 (a), where volumes are compared considering the final instant. A good agreement between the two approaches can be observed, with differences below 0.8% with the exception of the case γ=0.8 for which we obtained 2.4% deviation. Figure 7 (b) shows that the error increases with the sliding distance, particularly for the PoD case with γ=0.8, i.e. the lowest track radius. The reason for this highest error can be explained with the approximation of uniform contact pressure at the base of the analytical approach, as cleared below.

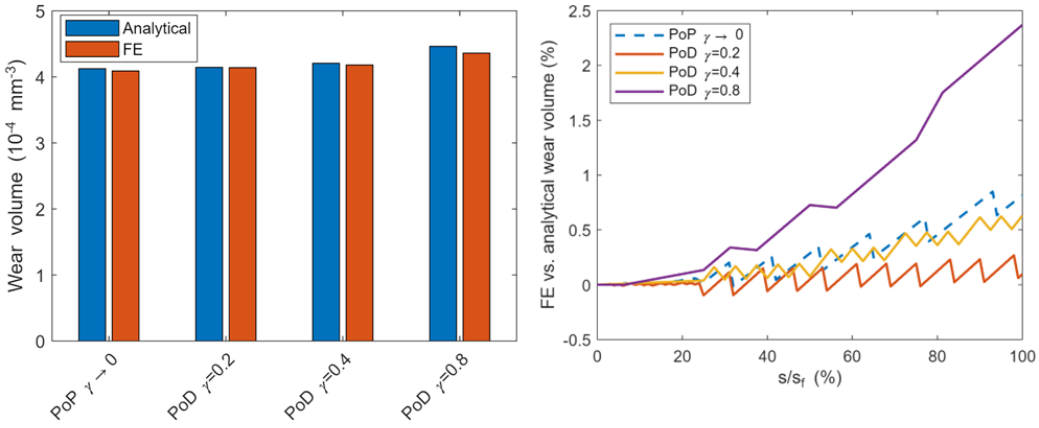

Figure 7. Comparison of the wear volumes predicted by the FE wear models and analytical formulations: (a) histograms of the final wear volumes, (b) errors in volume estimations between FE and analytical results. Final sliding distance s_f=157.08 mm.

The maps of the contact pressure at the same final sliding distance for the four examined cases are reported at the top of Figure 8. The maps of each case are shown both on the same scale (first row) and in its own full scale (second row) to highlight the main characteristics and ease the discussion. For the PoP test, the contact pressure was uniform over the contact area (with p=0.255 MPa), whilst it was not so in the PoD cases, which showed a pressure gradient, being the pressure higher in the region closer to the disk axis (at R_m), and lower far from it (at R_M). Additionally, the pressure gradient was more marked for higher values of γ, that means with the pin closer to the disk axis.

 doi:10.20944/preprints202403.0646.v1

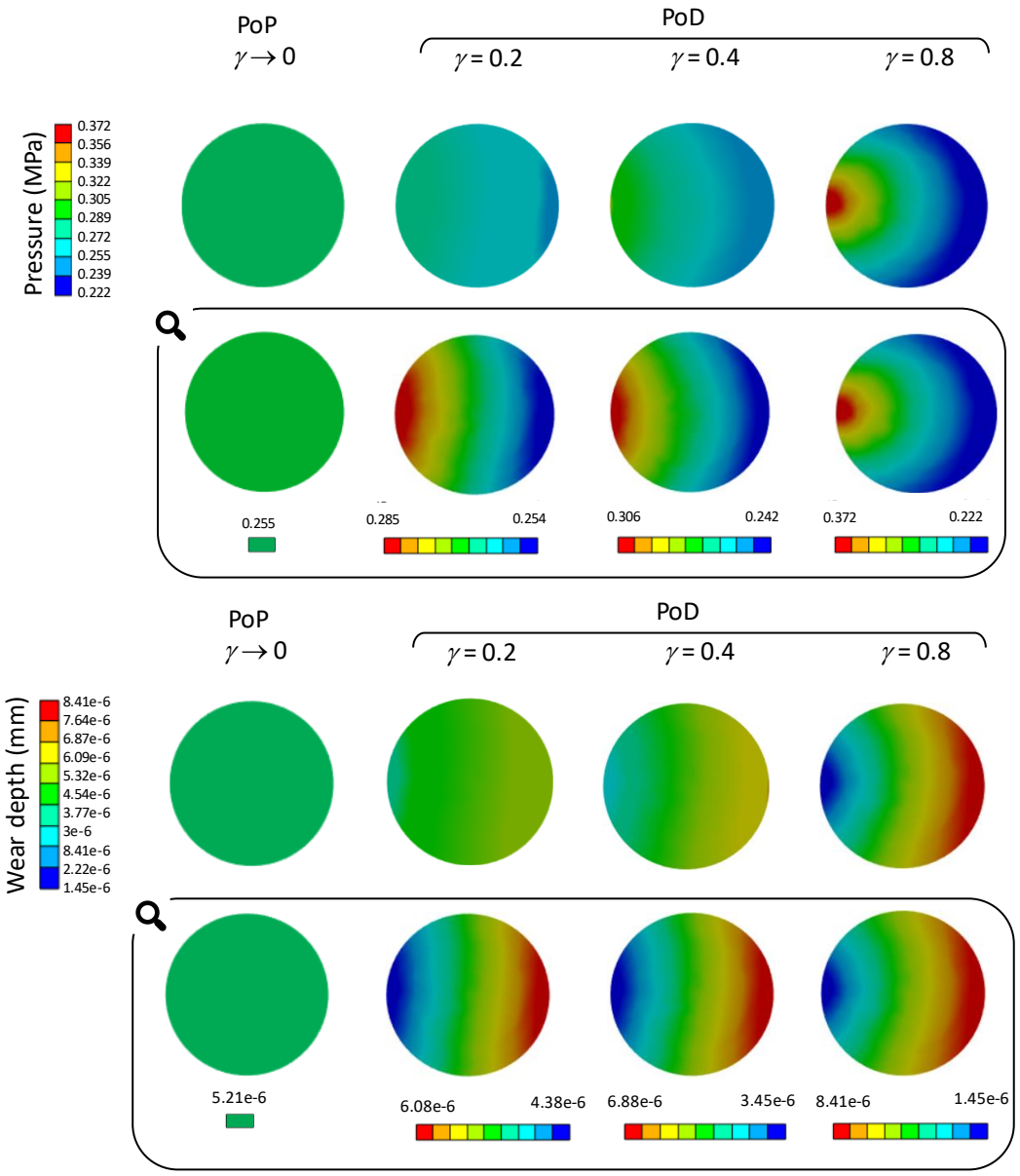

Figure 8. Maps of the contact pressure and wear depth in the four examined cases at the final sliding distance s_f=157.08 mm. For both pressure and wear depth, first row: all the cases are plotted with the same color band; second row: each plot in its color band. ($\gamma = 0.2, 0.4$ and 0.8 correspond to decreasing R_d= 5, 2.5 and 1.25 r_p, respectively).

In the case of PoP, the uniform contact pressure combined to uniform sliding velocity/distance over the pin surface, caused a uniform wear depth, as shown at the bottom of Figure 8. Differently, a gradient of the wear depth was predicted in all PoD cases, as opposite to the pressure one, with the minimum values at R_m and the maximum ones at R_M. As for the pressure, the gradient of the wear depth increased with γ values. At the end of the test, the surface was no more planar.

In order to fully understand the contact pressure and wear maps for the PoD tests, it is necessary to consider what happens during the wear tests, and thus their evolution with the sliding distance. For brevity, only the case γ=0.8 is detailed, being the most interesting and peculiar one. The evolution of pressure and wear depth during the simulation are reported in Figure 9 for 4 instants: in addition to the initial/unworn and final conditions, data at 1/3 and 2/3 s_f were considered. It can be observed that initially, pressure was uniformly distributed, as in the PoP case. During the test, a redistribution of contact pressure occurred, which can be explained considering the different sliding distance of the pin points: those farther from the disk axis describe a longer trajectory with respect to those nearer to

Preprints.org (www.preprints.org) | NOT PEER-REVIEWED | Posted: 11 March 2024 doi:10.20944/preprints202403.0646.v1

the axis. Consequently, the wear rate is higher on the outer part of the pin surface, which becomes curved, and this causes a pressure reduction. The trend of the maximum and minimum values of the contact pressure and the wear depth (h_{max}, h_{min}) with the sliding distance is well depicted in Figure 10. It can be observed that at the final sliding distance, the percentage pressure difference (p_{max}-p_{min}) with respect to the initial value $\underline{p}$ was of 57.6%, while the percentage difference of the wear depth (h_{max}-h_{min}) with respect to its average value (h_{max}+h_{min})/2 was of 141%.

This effect for which a higher sliding distance causes a reduction of pressure is expected to reach an equilibrium in a kind of stationary wear evolution that is not caught in the present simulation.

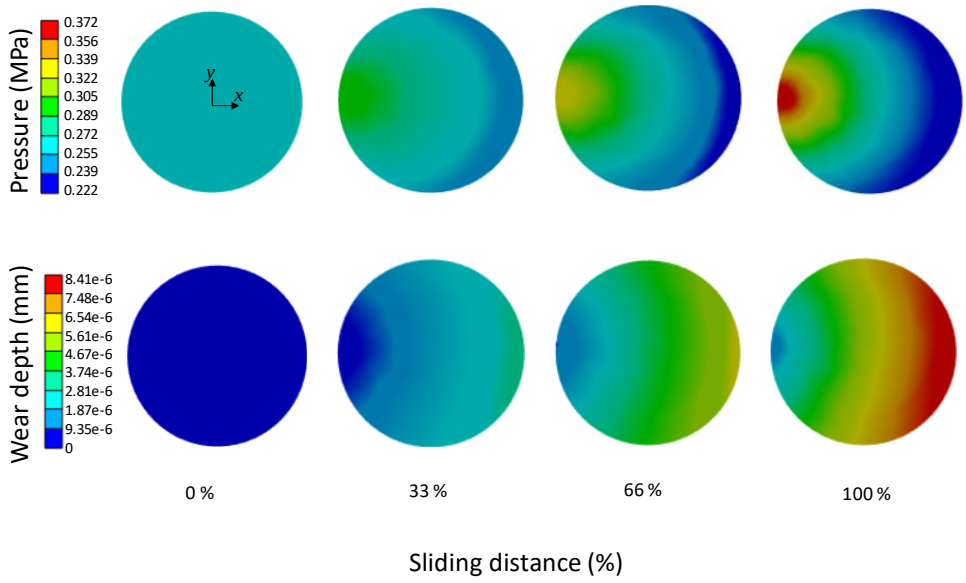

Figure 9. Evolution of the contact pressure (first row) and the wear depth (second row) over the contact area, with increasing sliding distance, from the left to the right. The final sliding distance s_f=157.08 mm corresponds to 100%. (PoD case with γ=0.8.)

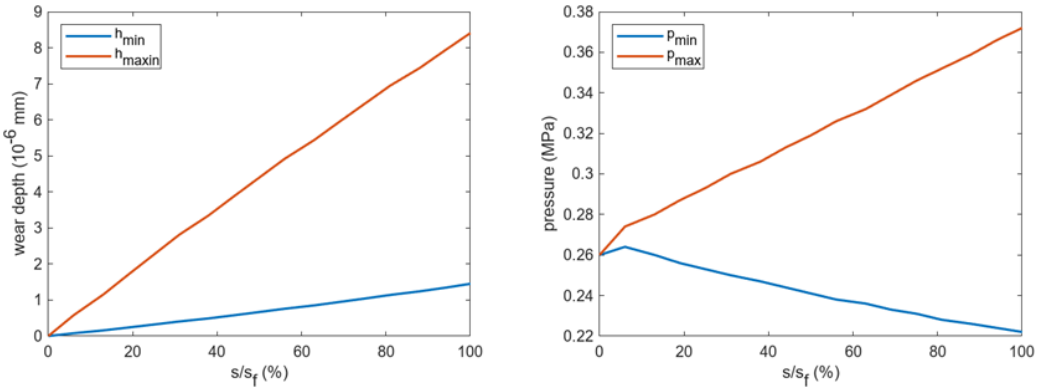

Figure 10. Evolution of the minimum and maximum wear depth and contact pressure with the sliding distance. Pressure is maximum when the wear depth is minimum and viceversa. (PoD case with γ=0.8.)

Similar considerations hold for all the PoD cases but in a more limited way, as proven by data in Table 1.

 doi:10.20944/preprints202403.0646.v1

Table 1. Gradient of pressure and wear depth at the end of the simulation for PoD cases. $\underline{p}$ is the initial contact pressure.

g	$\frac{p_{max}-p_{min}}{\underline{p}}$ 100	2 $\frac{h_{max}-h_{min}}{h_{max}+h_{min}}$ 100
0.2	12.1%	32.5%
0.4	25%	66.4%
0.8	57.6%	141%

4. Discussion

The wear behavior of a given material couple is typically described by a wear coefficient k that can be estimated from wear volume measurements in PoP and PoD tests, using the Archard wear law $k=V/(F\,s)$ (Eq.(2)).

The present study provides an analytical proof that Eq.(2) can be correctly applied to the PoP case, i.e. of a translating body under load, but is an approximation for the PoD one. Thus, differences between the two tests are deepened with an analytical and a FE approach, examining wear volume, wear maps and contact pressure in the first part, i.e. the transient phase, of the wear test. We considered four cases: one PoP and three PoD models with the pin placed at three different radii from the disc axis. Introducing a parameter $\gamma = r_p/R_d$, we distinguished the four cases as $\gamma \to 0$ (PoP), $\gamma =$ 0.2, 0.4 and 0.8 (PoD). FE analyses showed that wear volumes at the end of the test were different, increasing with γ from 4.09, 4.14, 4.18 to 4.36 10^{-4} mm^3 for the same load and sliding distance. These differences demonstrate that the use of Eq.(2) for PoD tests introduces an error which increases by reducing the distance between the pin and the disk axis (up to 6% for $\gamma = 0.8$), whilst tends to zero when the pin is far away from the disk axis, i.e. in conditions similar to the PoP. By means of an analytical approach, assuming a uniform pressure distribution also for PoD cases in the transient phase, a nondimensional function $g(\gamma)$ was introduced which provides an estimation of the wear volume in PoD vs. PoP for the same load and sliding distance. It can be approximated with a quadratic function

$$g(\gamma) \approx 1 + \left(\frac{32}{9\,\pi} - 1\right)\gamma^2 \quad \text{for } 0 \le \gamma \le 1 \tag{17}$$

stating that the ratio is higher for higher γ, i.e. when the pin is closer to the disk axis.

Analytical and FE approaches provided very similar wear volumes with percentage differences lower that 2.4%, higher for the PoD with $\gamma = 0.8$, i.e. when the pin is placed near to the disk axis. Such differences are caused by the assumption of a uniform contact pressure adopted in the analytical formulation, while plots in Figure 9 clearly show that this is true at the beginning but it is not the case at the end of the test, as confirmed by Table 1. However, in the present case such an assumption affects wear estimation only marginally.

It is worth stressing that the standard ASTM G99 suggests a track radius R_d within the range 12.5-17.5 mm for a pin with $r_p = 5$ mm, as in the present case, corresponding to $0.286 \le \gamma \le 0.4$. Actually, the standard suggests a spherical head for the pin so that the contact area is very small (initially) and the case is equivalent to $\gamma \to 0$. Until wear causes an important increment of the contact area, for a PoD test with a spherical pin Eq.(2) can be applied. An estimation of the extension of the contact area may be obtained through the simple formulation proposed by these authors in [16,17].

The FE investigation of the evolution of pressure and wear depth clarified the role of the sliding distance on pressure redistribution with time. It was observed that contact pressure, initially uniform, tends to increase close to the disk axis and decrease far from it, while its integral remains the same, corresponding to the external load. Indeed, the pin surface undergoes to higher sliding distances in the outer region, compared to the inner one, and thus higher wear. Similarly wear depth evolves but

 doi:10.20944/preprints202403.0646.v1

in an opposite way with respect to pressure gradient. Interestingly, the pin surface is no more planar, although, thanks to elastic deformations, it comes fully into contact with the disk surface under load.

However, as mentioned above, this study is focused on the transient phase of the wear process while a steady phase is expected to be achieved at longer sliding distance. Since very small time increments were necessary to describe the circular trajectories of points, the computational cost of the proposed simulations was rather high. To complete the study with the steady state phase, strategies for accelerating simulations are going to be pursued.

In conclusion, the present study highlights the need to deepen the methodology for k estimation, not described in standard ASTM [1,3]. The rotational effect in PoD tests, which varies with the distance between pin axis and disk axis and even change during the wear process in case of spherical pin tip, should be considered in k estimation. Its neglection could explain in part the high data dispersion of k values reported in experimental studies. The hypothesis of a constant k should be taken with cautions even for metallic materials traditionally used in tribo-couples, and the real contact conditions should be considered in its estimation particularly for plastic materials such as the UHMWPE characterized by cross-shearing [7]. Such aspects are going to be tackled in future studies.

Author Contributions: Conceptualization, F.DP. and L.M.; methodology, F.DP. and L.M.; software, A.DP.; validation, F.DP.; formal analysis, F.DP. and L.M.; data curation, A.DP.; writing—review and editing, F.DP. and L.M.; funding acquisition, F.DP. All authors have read and agreed to the published version of the manuscript.

Funding: National Recovery and Resilience Plan (PNRR), Mission 4, Component 2, Investment 1.4, "National Centre for HPC, BigData and Quantum Computing", European Union-Next Generation EU.

Data Availability Statement: The data presented in this study are available on request from the corresponding author.

Conflicts of Interest: The authors declare no conflicts of interest. The funders had no role in the design of the study; in the collection, analyses, or interpretation of data; in the writing of the manuscript; or in the decision to publish the results.

References

1. G02 Committee ASTM G99 - Test Method for Wear Testing with a Pin-on-Disk Apparatus.
2. ASTM D4170-16 Standard Test Method for Fretting Wear Protection by Lubricating Greases.
3. ASTM G133 - Standard Test Method for Linearly Reciprocating Ball-on-Flat Sliding Wear.
4. Liu, H.; Chen, Y.; Wang, X.; Guo, Y.; Xue, W.; Li, D.; Chen, X.-Q. Correlating Numerical Modelling with Experimental Studies to Quantify the Wear Resistance of High-Carbon Chromium Bearing Steel in Mixed Lubrication. *Tribology International* **2023**, *188*, 108819, doi:10.1016/j.triboint.2023.108819.
5. Bastola, A.; McCarron, R.; Shipway, P.; Stewart, D.; Dini, D. Experimental and Numerical Investigations of Sliding Wear Behaviour of an Fe-Based Alloy for PWR Wear Resistance Applications. *Wear* **2024**, *540–541*, 205186, doi:10.1016/j.wear.2023.205186.
6. Mattei, L.; Di Puccio, F. How Accurate Is the Archard Law to Predict Wear of UHMWPE in Hard-on-Soft Hip Implants? A Numerical and Experimental Investigation. *Tribology International* **2023**, *187*, 108768, doi:10.1016/j.triboint.2023.108768.
7. Mattei, L.; Di Puccio, F.; Joyce, T.J.; Ciulli, E. Numerical and Experimental Investigations for the Evaluation of the Wear Coefficient of Reverse Total Shoulder Prostheses. *Journal of the Mechanical Behavior of Biomedical Materials* **2016**, *55*, 53–66, doi:10.1016/j.jmbbm.2015.10.007.
8. Archard, J.F. Contact and Rubbing of Flat Surfaces. *Journal of Applied Physics* **1953**, *24*, 981–988, doi:10.1063/1.1721448.
9. Lancaster, J.K. The Influence of Substrate Hardness on the Formation and Endurance of Molybdenum Disulphide Films. *Wear* **1967**, *10*, 103–117, doi:10.1016/0043-1648(67)90082-8.
10. Matkovič, S.; Pogačnik, A.; Kalin, M. Wear-Coefficient Analyses for Polymer-Gear Life-Time Predictions: A Critical Appraisal of Methodologies. *Wear* **2021**, *480–481*, 203944, doi:10.1016/j.wear.2021.203944.

11. Borawski, A. Testing Passenger Car Brake Pad Exploitation Time's Impact on the Values of the Coefficient of Friction and Abrasive Wear Rate Using a Pin-on-Disc Method. *Materials* **2022**, *15*, 1991, doi:10.3390/ma15061991.
12. Bastola, A.; Stewart, D.; Dini, D. Three-Dimensional Finite Element Simulation and Experimental Validation of Sliding Wear. *Wear* **2022**, *504–505*, 204402, doi:10.1016/j.wear.2022.204402.
13. Reichelt, M.; Cappella, B. Large Scale Multi-Parameter Analysis of Wear of Self-Mated 100Cr6 Steel – A Study of the Validity of Archard's Law. *Tribology International* **2021**, *159*, 106945, doi:10.1016/j.triboint.2021.106945.
14. Põdra, P.; Andersson, S. Simulating Sliding Wear with Finite Element Method. *Tribology International* **1999**, *32*, 71–81, doi:10.1016/S0301-679X(99)00012-2.
15. Mattei, L.; Di Puccio, F. Frictionless vs. Frictional Contact in Numerical Wear Predictions of Conformal and Non-Conformal Sliding Couplings. *Tribol Lett* **2022**, *70*, 115, doi:10.1007/s11249-022-01657-5.
16. Di Puccio, F.; Mattei, L. Simple Analytical Description of Contact Pressure and Wear Evolution in Non-Conformal Contacts. *Tribology International* **2023**, *178*, 108084, doi:10.1016/j.triboint.2022.108084.
17. Di Puccio, F.; Mattei, L. Further Validation of a Simple Mathematical Description of Wear and Contact Pressure Evolution in Sliding Contacts. *Lubricants* **2023**, *11*, 230, doi:10.3390/lubricants11050230.